Assessing the effects of urbanization on land use land cover changes and land surface temperatures in Sejong, South Korea

Eun Hye Grace Choi

Advisor: Professor Jennifer J. Swenson

April 22, 2022

Masters project proposal submitted in partial fulfillment

of the requirements for the Master of Environmental Management degree

in the Nicholas School of the Environment of

Duke University

Executive Summary

The capital of South Korea, Seoul, occupies only 0.61 percent of the country's land area, yet the metropolitan area is home to more than 50% of the country's people. Acknowledging this demographic imbalance, the Sejong special autonomous city was established on July 2, 2012, with the majority of central government ministries and public organizations relocating to Sejong. In reaction to the master-planned city's implementation, Sejong's ongoing development has prompted criticism and raised several environmental concerns. One major environmental consequence of urbanization is the urban heat island effects. Urban heat islands (UHI) result from replacing natural landscapes with dense concentrations of pavement and other surfaces that absorb and retain heat, resulting in greater temperatures than outlying rural areas and a negative influence on people's health. To make things worse, the convergence of ongoing climate warming and urban heat island effects is also increasing inequality as low-income neighborhoods have less tree cover, more concrete and asphalt that absorb and retain more heat (O'Brien, 2021).

Sejong, with its fast and high-density urbanization, presents itself as a useful case for examining the UHI effect in a newly built city. With countries increasingly relocating cities and administrative centers, whether due to pollution, over-population, or flooding risk, it is crucial to understand the experiences of nations that have completed the shift, allowing the formulation of suitable policy measures for smarter and more sustainable development.

Thus, this research examines the effects of land-use/land-cover (LULC) changes on land surface temperatures (LSTs) over a 12-year timespan for a capital city built from the ground up using Landsat 5, 8, and MODIS remotely-sensed imagery. To observe correlations between land-use percentage coverage and surface temperatures, the LST and land-use classification mapping for the full study area is derived from Landsat imagery in summer dates of 2004, 2009, 2013, and 2020. This study also explores the relationship between increased LST intensity and urban growth, as well as changes in greenness (NDVI: Normalized Difference Vegetation Index) as a result of translating MODIS' monthly raster values into a time series for a number of different places that have undergone both more and no urbanization. Furthermore, the current study aims to determine changes of LULC and their impacts on the UHI intensity in different urban areas by using LST

data collected in 2020 and linking it to indices that mark different urban features. Finally, LSTs of different LULC were analyzed both during the daytime and nighttime using ECOSTRESS.

The findings for LULC analysis show that the amount of built-up area increased considerably from 2004 to 2020 (34%). In addition, the LULC analysis results demonstrate that the urban expansion witnessed in Sejong was due to the conversion of agricultural land (-43%) to built-up land. From 2004 to 2020, LST ranges were 21-34°C in 2004, 24-39°C in 2009, 16-40°C in 2013, and 23-47°C in 2020, indicating a significantly increasing trend. In addition, between 2004 and 2020 there was an increase in study area mean LST from 25.69°C to 35.89°C. Overall, a correlation between the greatest LST increases and increased land development was observed, while the lowest LST represented non changing vegetation cover. Additionally, the LST maps reveal that high LST values are concentrated in the most populous towns of Sejong. It was found that typical LSTs for the populous towns range between 30 to 43° C for the summer months in 2020.

The mean NDVI for the non-changing rural and urban conversion areas was 0.5 and 0.24, respectively. While the rural areas did not experience any class changes, the NDVI decreased significantly over time in the urban area, therefore there is a significant decrease in the NDVI difference between rural and developing beginning in 2010, which is consistent with the start of construction in 2011. However, based on these results, we can see that despite the impervious nature of the urban area, there is still some greenness, consistent with the design of the city, which incorporated green roofs among other environmental strategies. The gradient of UHI intensity analysis indicates that urban areas experienced a 1.92°C higher LST on average compared to rural areas. The strongest UHI demonstrated a 3.38°C higher LST and -0.449 lower NDVI compared to the rural areas. According to the Kendall correlation test, the UHI and NDVI differences have a negative correlation of 0.55 (Kendall correlation test).

The time of day exhibited different effects of ECOSTRESS-derived LST depending on different land features. The contrast in LST distribution among land features was greater at 10:14 a.m. and more stable at 4:43 p.m. Under the effect of daytime sunlight, settlements and bare soil have the fastest temperature increase at 10:14 a.m. and is defined by a comparatively warmer temperature than other land class.

Lastly, the mean LST results in 2020 indicate that urban heat island intensity varied among cities with very similar NDVI results. Dajung-dong, situated at the center of Sejong city and very far from a river or forest, had the highest temperature. Meanwhile, the coolest temperature was found in Eojin-doing, where the government complex is located, highlighting the potential solution of green roofs as a way to mitigate increased temperatures in cities. Consequently, special measures should be taken to alleviate the UHI effect in the city center or parts of the city expected to have unusually high number of heat-absorbing pavements.

Assessing the effects of urbanization on land use land cover changes and land surface temperatures in Sejong, South Korea

Table of Contents

1. Introduction

Background

Urban population in 2019 accounted for 55.7% of the world's population, up from 29.6% in 1950- a proportion that is expected to increase to 68% of the world population by 2050. (The World Bank, 2019; WHO). Urbanization is inevitable, and urban development forms a fundamental basis for the majority of endeavors and functions that support innovation and economic advancement (Adedibu, 1987).

However, as a result of rapid urbanization and industrialization, numerous environmental problems and health implications of these environmental problems have emerged (Kim & Baik, 2005). These problems include elevated daytime temperatures, reduced nighttime cooling, emissions of air pollutants, impaired water quality, and solid waste management problem, which have a serious toxicological impact on human health and the environment (Balali-Mood, et. al, 2016; PBR, 2004; Seoul Solution, 2016).

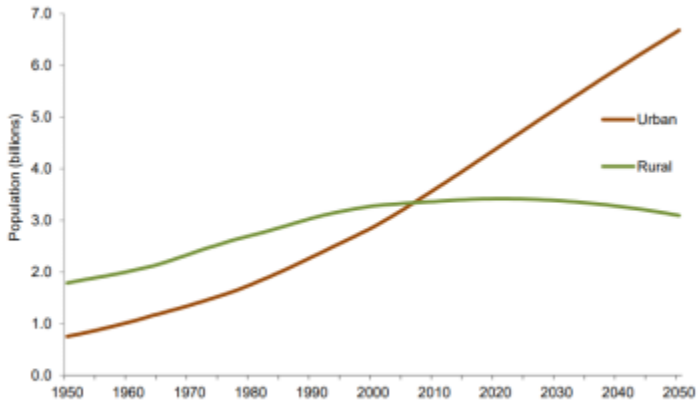

Figure 1. Urban and Rural Populations of the World, 1950-2050 (OECD)

The city of Seoul is the capital of South Korea, its biggest metropolis, and the 16th largest city globally (ESA, 2017). Although it covers a mere 0.61% of national territory, the metropolitan area is home to half the country's population. In 2004, the Government of Korea took steps to deal with the clustering around the capital. Following a three-phase plan that Sejong would become a special administrative city, most government bodies, including 36 ministries and 10,452 civil servants, relocated there from Seoul since 2012.

This has necessitated the rather rushed construction of a self-sustaining city on what had previously been agricultural land. Initially, civil servants who had been relocated to Sejong could only access one small supermarket and the nearest health facilities were in a neighboring city. As of 2020, Sejong's population is 351,007-a remarkable increase from the 80,031 recorded in 2000. Still under development, the city is planned for completion by 2030 (Sejong City).

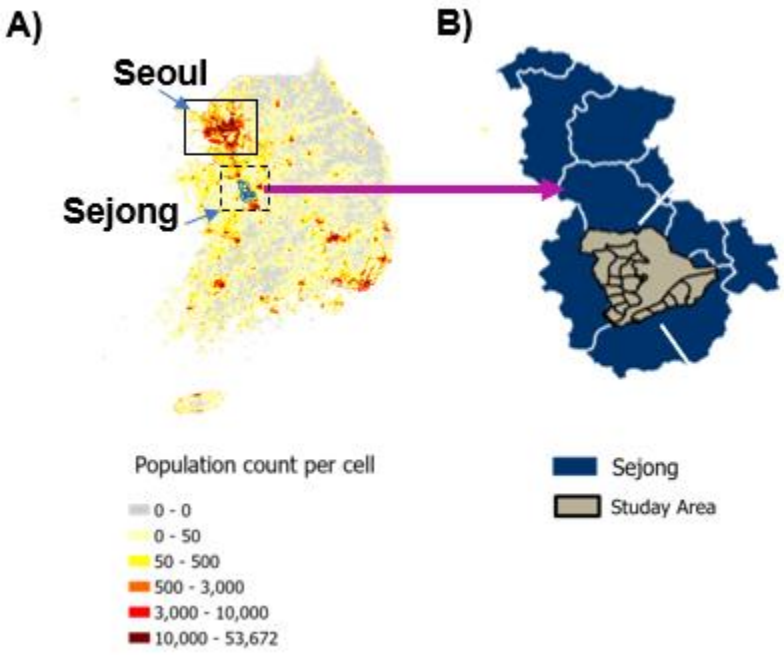

Figure 2. (a) The image on the left is a map of South Korea. The black solid line borders Seoul, while the dashed line borders Sejong. (b) The image on the right is a map of Sejong, which is colored blue. The study area, colored brown, in confined to the middle of Sejong.

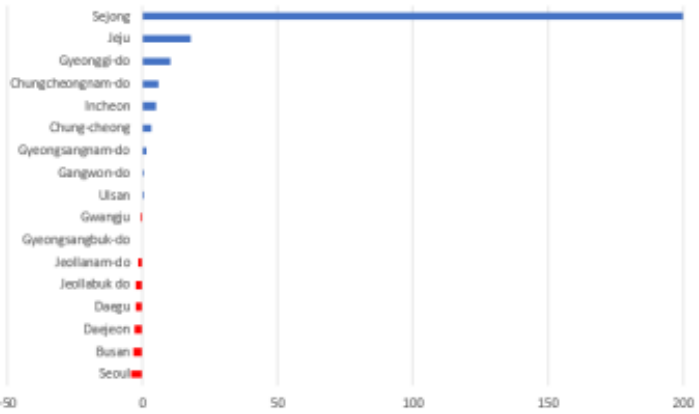

Figure 3. Largest cities of South Korea's population growth rate % (2019 compared to 2012) (Data.GO.KR)

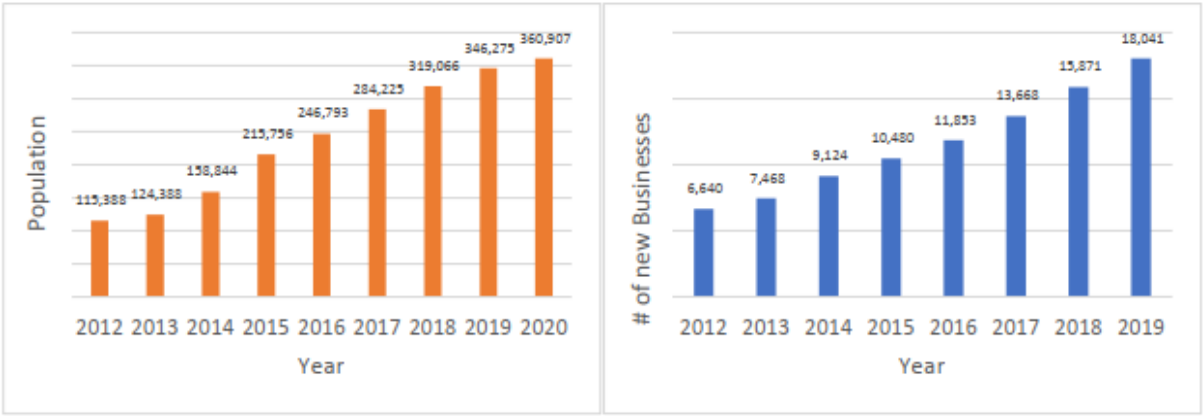

Figure 4. Charts of population level (left)/ businesses (right) in Sejong from 2012 to 2020 (Data.GO.KR)

Urban Heat Island

Light and heat from the sun reach the country and city in the same way. Differences in the temperature observed in urban and rural areas can be attributed to the extent to which the surfaces in each respective environment take in and maintain heat (National Geographic Society, 2012). Several developments within the urbanization process cause a gradual increase in the air temperature within the city. These include the replacement of natural landscapes by artificial structures with impervious surfaces and a reduction of vegetation biomass, which in turns alters the absorption, storage, and emittance of energy (EPA, 2020; Marial et al., 2013; UCAR; Yoo,

2019). Hence, the area has witnessed rising surface temperatures and the emergence of a so-called urban heat island (UHI), a micro-climate increasingly seen in urban areas of this type, which leads to higher temperatures and lower air quality (EPA, 2020).

Urban heat islands occur when a city experiences higher temperatures than nearby rural areas. UHI can be influenced by a range of factors, including road traffic intensity, climate characteristics, geographical location, urban population, and the way in which heating and cooling energies are distributed and consumed (Tzavali et al, 2015). Oke (1973) and Park (1986) presented functional relations that correlated the intensity of an UHI with population. Ichinose et al. (1999) demonstrated that the urban heat island intensity is at its highest in winter because anthropogenic heat has relatively greater impact during this period. As such, one of the leading causes of urban heat island today is urbanization/anthropogenic heat (Appleton, 2020).

These, in turn, exacerbate the risk of heat-related mortality associated with global climate change (Manoli, 2019; Marial et al., 2013). It also contributes to heat-related illnesses such as respiratory difficulties and heat exhaustion (EPA, 2020). Higher daytime temperatures and reduced nighttime cooling can cause general discomfort. Prolonged exposure to extreme heat is a key driver of health risk in the world today, especially to seniors and females (Wang et.al, 2021). Sustained heat builds heat stress and impacts the human body that allows it to adjust to heat become overwhelmed (Harmon, 2010).

To make things worse, the urban heat island effects compounded by climate warming are also increasing inequality as low-income neighborhoods have less tree cover, more concrete and asphalt

that absorb and retain more heat (O'Brien, 2021). Vulnerability to urban heat varies across urban communities associated with existing socioeconomic and demographic factors (Li et al., 2008; Chakraborth et al., 2019). According to the lead scientist at the Nature Conservancy, it is estimated that the lower-income neighborhoods than those in the surrounding area have approximately 54 percent less tree cover and are 5°C hotter on average.

Objective

Sejong, with its fast and high-density urbanization, presents itself as a useful case for examining the UHI effect in a newly built city. With countries increasingly relocating cities and administrative centers, whether due to pollution, over-population, or flooding risk, it is crucial to understand the experiences of nations that have completed the shift, allowing the formulation of suitable policy measures for smarter and more sustainable development.

Hence, this project assesses how land-use/land-cover (LULC) changes impact land surface temperatures (LSTs), specifically in a newly constructed planned city. The aim hereby is to investigate how the relocation of high-density areas influences UHI intensity. Thus, the objectives are to evaluate the magnitude of the LULC changes in the planned city of Sejong, the consequential impact on UHI intensity and greenness, and the interactions between them. Furthermore, I examine the variation in trends of LSTs in different land features and pay special attention to the different climate sensitivities of land features during the daytime and nighttime using ECOSTRESS-retrieved LST images over Sejong, Korea.

Literature Review

Yoo et. al (2019) analyzed the urban heat island in Sejong utilizing surface temperature change values from Landsat 8 and NDVI (Normalized Difference Vegetation Index) and NDVI based on KOMPSAT 2 data. Their results show that hot spots appeared in urbanized regions within the study area, and it was plotted that lower NDVI values indicate higher temperature values. The main limitations of the previous study are that it didn't examine an urban environment in a detailed manner; rather, it was focused on the correlation between LST and NDVI/NDBI in discrete time series as opposed to considering the relationship between LST and LU/LC. According to Boo and Oh's (2000) observations, an area of relative warmth can be seen in the central area of the city, which is densely built-up. This warmth is directly related to the topography of the land and how it is used. This study will draw from the work of Hoan (2019), Aik et. al. (2020), Pal and Ziaul (2017), Quan (2016) by studying LST between various LULC forms in Sejong.

2. Methods

2.1 Study Area

Founded in 2007, South Korea's new administrative city of Sejong is the country's smallest first-level administrative division, covering only 465.23 km^2. It is set to become South Korea's new administrative city, with planners aiming to address the congestion problems that have plagues its current capital as well as decentralize power and promote more development opportunities outside the nation's largest city. Following the decision, the South Korean government initiated the move of its capital in 2012 and has been moving various agencies and ministries to Sejong since then.

Since that date, the Sejong area has undergone rapid urbanization and a massive, approximately 350 percent, population growth from 80,031 in 2010 to 360,907 in 2020 (Sejong City).

Located around 120km (about 74.56 miles) to the south of Seoul and encompassing some parts of the South Chungcheong and North Chungcheong provinces, Sejong lies at the country's center. The self-governing city division is long and narrow, runs from north to south, and comprises two previously developed areas, separated by the Charyeong Mountain Range and the Geumgang River. It is divided into 9 myeon (townships), 1 eup(town), and 12 haengjeong-dong (administrative neighborhood). The area under study is not Sejong as a whole but rather the administrative districts, encompassing around 77.92 km^2, as this is where rapid urbanization is happening (Figure 5).

Situated 15.27 meters above sea level, Sejong has a humid continental climate with hot summers and very dry winters. On average, Sejong received around 50.06 millimeters of rainfall annually, with 84.07 rain days (23.03%) (Weather and Climate).

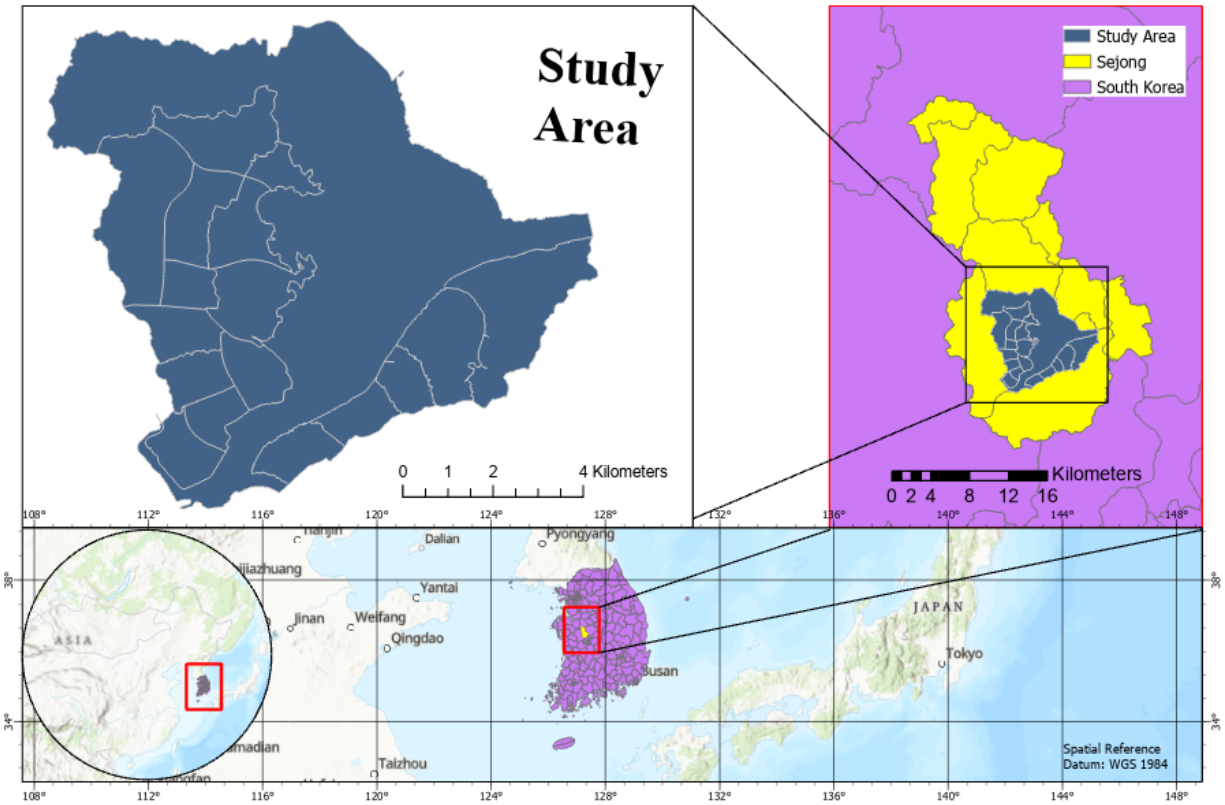

Figure 5. Location of the study area: (Top left) The study area for this study. (Top Right) The map of Sejong. (Bottom) The map of South Korea, which is colored purple.

2.2 Remote Sensing Image Acquisition

LST and LULC

LULC

To assess the magnitude of LULC change from the master-planned city, the land-use classification mapping for the full study area is retrieved from imageries collected by Landsat 5 and 8 in four summer dates: 2004, 2009, 2013 and 2020. The four dates were selected based on images with cloud cover less than 5% and similarities in the air temperature observed at two meteorological stations bordering Sejong and in the temperature of the pixels at the middle of the river because these are the most unaffected pixels and maintain a constant temperature (Figure 6; Listed in Table 1). This avoids bias due to hotter days and provides a more comparable trend to discern changes in the temperature trend over time, which is essential to any change detection analysis.

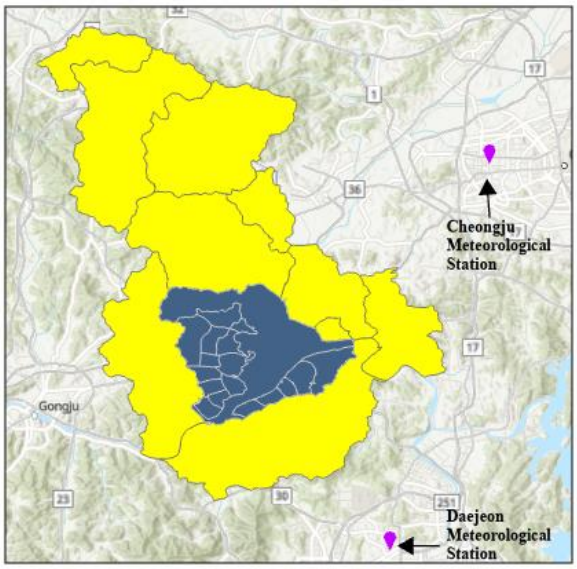

Figure 6. The locations of the two meteorological stations bordering Sejong

	Air Temp (°C) Cheongju @ 1 PM	Air Temp (°C) Daejeon @ 1 PM	Air Temp (°C) Sejong @ 1 PM
2004-08-31	28	27.6	Unavailable
2006-08-05	31.7	32	Unavailable
2008-09-18	30.1	29.8	Unavailable
2009-06-26	29.4	28.1	Unavailable
2011-09-27	25.2	24.4	Unavailable
2013-06-05	29.7	29.9	Unavailable
2014-05-30	30.8	30.8	Unavailable
2015-07-04	27.8	27.3	Unavailable
2017-06-16	29.7	30.6	Unavailable
2019-06-13	27.8	28.6	27.6
2020-06-08	30.1	30.5	29.3

Table 1. Sejong's air temperature from the meteorological stations from 2004-2020

Description of Land use land cover categories

The classification scheme includes four land-use/land-cover types: water body, built-up area, vegetation, and agriculture (Table 2). Land use/Land Cover Changes information for the study area

was interpreted from Landsat images acquired from the summers of 2009 to 2020, using the supervised object-based image classification. In supervised image classification, around 20 samples for each class were used to train classifiers. To ensure that the landcover was correctly classified, accuracy analysis was performed on the classified images from Google Earth time series images and Environmental Geographic Information System developed by the Ministry of Environment of South Korea. After verifying that the accuracy level was above the acceptable 85% threshold, the mean LST was calculated for the different land features.

Land Cover Types	**Description**
Vegetation/Forest	Tree cover and vegetative crops
Developed/Barren	Settlement areas, asphalt cover (roads, parking lots, and industries) Bare soil surface without any cover
Water	Water features
Agriculture	Farming land

Table 2. Description of land use/cover categories

Land Surface Temperature Calculation

Available Landsat images were collected for the study area for the summers from 2004 to 2020, and the land surface temperatures were calculated at 30m resolution imagery by using ArcGIS.

The study was limited to summer temperatures to realistically capture the details of intense urban heat islands. Land surface temperature for this study is retrieved using the Radiative Transfer Equation method and the emissivity method developed by Sobrino et al. (2008). According to Sekertekin (2020), Sobrino et al. (2008)'s emissivity method for the RTE (2.85 RMSE) presented the best result. This study draws work from Sekertekin and Bonafoni (2020) to develop more in-depth insights into the spatial characteristics of Sejong's UHI by testing out different LST retrieval methods.

Radiative Transfer Equation and Sobrino's emissivity methods:

1. Mean effective atmospheric temperature retrieval (T_a) using near-surface air temperature (T_o). Model: mid-latitude summer region. $T_a = 16.011 + 0.9262 * T_o$
2. Atmospheric transmittance, upwelling radiance, and downwelling radiance were obtained from NASA's atmospheric correction parameter calculator.
3. RTE:

$$L_\lambda^{sen} = \left[\epsilon B_\lambda(T_s) + (1-\epsilon)L_\lambda^{\uparrow}\right]\tau + L_\lambda^{\uparrow}$$

L_λ^{sen}	At-sensor registered radiance of the related thermal band
B_λ	Blackbody radiance
$B_\lambda(T_s)$	Blackbody radiance at a temperature of T_s
T_s	Obtain by inverting Planck's law

4. Sobrino's emissivity (NDVI threshold-based LSE model)

$$\epsilon = \begin{cases} a_i \rho R + b_i \\ \epsilon_V + \epsilon_S(1-P_V) + d\epsilon, \;\; d_\epsilon = (1-\epsilon_S)(1-P_V)F_{\epsilon_V} \\ \epsilon_V + d_\epsilon \end{cases}$$

$$\begin{matrix} NDVI < 0.2 \\ 0.2 \leq NDVI \leq 0.5 \\ NDVI > 0.5 \end{matrix}$$

$NDVI < 0.2$: bare soil; $NDVI \leq 0.5$: bare soil and vegetation; $NDVI > 0.5$: fully vegetated areas

a_i	$a_i = .979; b_i = .035$
b_i	channel dependent regression coefficients from the red band reflectance and MODIS emissivity library
ρR	reflectance value from the red band
ϵ_V, ϵ_S	vegetation and bare soil emissivity from MODIS emissivity library
d_ϵ	cavity effect due to surface roughness, $0 =$ for flat surface
P_V	the proportion of vegetation cover
F	geometrical shape factor

Validation of Landsat-derived LST retrievals is performed to the ground-based LST measurements at two meteorological stations bordering Sejong at 1pm. Landsat's scene center time for the study area varies between 1 and 2pm (local time).

	Ground surface temperature °C (10cm above ground)			**Landsat-derived LST °C**
	Cheongju	**Daejeon**	**Sejong**	**Mean LST of study area**
2004-08-31*	30.1 @ 3pm	30.6 @ 3pm	Unavailable	25.7 @ 1pm
2009-06-26 @1pm	30.5	30.8	Unavailable	29.5
2013-06-05 @1pm	27.6	30.4	Unavailable	30.2
2020-06-08 @1pm	Unavailable	27.6	41.8	38.9

Table 3. Ground-based LST measurements at two meteorological stations bordering Sejong (KMA)
*** 1pm ground surface temperature is unavailable for 2004-08-31**

LST and NDVI

MODIS

Construction on the city first began in 2006; thus, to consider UHI continuously over time, the monthly averages for remote-sense LST and NDVI (Normalized Difference Vegetation Index) with 1-km spatial resolution between 2004 and 2020 are extracted from MODIS. While its resolution is not as spatially fine as the Landsat data, MODIS offers enhanced temporal resolution, making it optimal for research using continuous time-series datasets. This study examines specific areas of interest to assess how urbanization affects UHI intensity; thus, it focuses on pixels that represent rural and urban areas rather than considering the entire area as a whole. Urban area was hereby defined as built-up land in areas that had the highest population count per cell in 2020, while rural area was identified as a vegetated area with no land class changes and situated no more than 5 km from an urban area.

This study aims to assess how UHI intensity is affected by city construction over time. Thus, to gain insight into the overall trend in land development's effect on LST, the study follows Quan et. al (2016) and defines UHI intensity as the difference between the average temperature of the urban and rural area in terms of the decomposed trend as well as the seasonal components in the MODIS time series.

UHI intensity = Urban conversion – Rural averages of the decomposed trend/seasonal component

Greenness difference = Urban Conversion – Rural averages of the decomposed trend-seasonal component

Nighttime LST/LULC

ECOSTRESS/Landsat

Landsat 8 data from 2019 (June) were acquired over the region of interest for LULC component at 30-m resolution imagery. The classification scheme includes four land use types: water, settlements, vegetation, and barren. The mean LST was calculated for the different LULC components after verifying the accuracy of the classified images.

The day and night LST images of Sejong, South Korea were obtained at a 70-m resolution from NASA's ECOSTRESS thermal infrared remote sensing data in the Level-2 product (ECOSTRESS Version 1), including quality control for LST and emissivity. The acquisition time for June in 2019 was at 10:14am and 4:43pm. An extensive amount of time was spent looking at the quality assurance information to determine the usefulness of the LST and emissivity data. Data with the least intervals between daytime and nighttime LST data, with the least percent cloud cover, and

with the high percent good quality data were selected for this project and extracted by using ArcGIS.

3. Results and Discussion

3.1 Land Change Analysis

The magnitude of LULC change of the master-planned city

The produced 30-m resolution land use maps of Sejong for the years 2004, 2009, 2013, and 2020 are displayed in Figure 8 (Top). As the Landsat 30-m resolution of Landsat 5 is subject to limitations, it was not possible to classify the finer details; thus, the distinction between developed land and barren land could not be made. A comparison between the 2004 and 2013 land use maps clearly shows the rapid rate of urbanization. Specifically, a significant change of 34% was seen for agriculture land class, while a 24% increase was observed for developed/barren land. This rapid expansion of urbanization and the degradation of agricultural land continued until 2020. In addition, the LULC analysis results demonstrate that the urban expansion witnessed in Sejong was due to the conversion of agricultural land to build-up land. In 2004, the largest recorded class was primary agriculture (46% of total area), followed by vegetation. However, agriculture land was the minor recorded class in 2020. The 11% increasing changes of vegetation body areas is perhaps due to regrowth of forests from abandoned farmland.

	2004 Area (%)	2009 Area (%)	2013 Area (%)	2020 Area (%)
Agriculture	46	41	7	3
Developed/Barren	16	23	47	50
Water	5	4	5	4
Vegetation	33	33	41	44

Table 4. Percentage distribution of each LULC type for the study area during the period under study

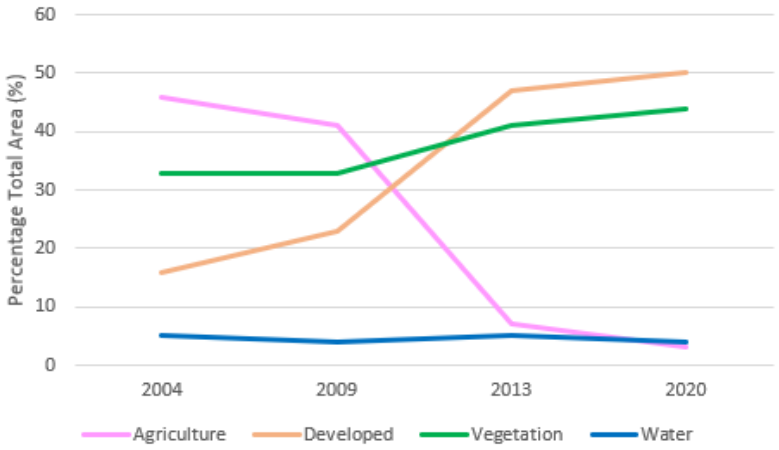

Figure 7. Comparing the spatial-temporal changes in 4 LULC types between 2004 and 2020

3.2 Land Surface Temperature Change Analysis

Figure 8 shows LULC maps of Sejong for 2004, 2009, 2013, and 2020, and their corresponding LST maps, respectively. These results show that LST ranges were 21-34°C in 2004, 24-39°C in 2009, 16-40°C in 2013, and 23-47°C in 2020, indicating a significantly increasing trend. In addition, between 2004 and 2020 there was an increase in study area mean LST from 25.69°C to 35.89°C. Table 5 presents the mean LST for each LULC class for 2020. As per the results, the highest and lowest LST respectively correlate with the developed/barren land class and the vegetation class. From 2004 to 2020, the developed land class experienced a 4°C increase in LST between 2004 and 2013, although there was a 1° C decrease from 2004 to 2020. This could be attributed to the use of a different Landsat in 2020 compared to 2004 or not differentiating the difference between developed and barren land class. The vegetation class experienced an increase in mean LST from 26 °C to 34°C between 2004 and 2020.

Overall, a correlation between the greatest LST increases and increased land development was observed, while the lowest LST increase represented non changing vegetation cover. This finding is in line with those of prior studies on cities in other country contexts (Maskooni et. al, 2021). This is also consistent with prior studies that demonstrated lower temperature in areas with green cover as it absorbs and reflects radiation while influencing the exchange of both latent and sensible heat (Maskooni et. al, 2021). Many studies associate this with the high levels of evapotranspiration by the vegetation, which reduces the surrounding temperature (Maskooni et. al, 2021). The spatiotemporal variation in LST correlates with the expansion of urban areas and the variation in LULC variation, thereby influencing the city's UHI effect. Additionally, the LST maps reveal that high LST values are concentrated in the most populous districts of Sejong. It is found that typical LSTs for the populous towns range between 30 to 43° C for the summer month in 2020.

	LULC changes between years 2004 and 2020	**Mean LST (2020) Celsius (°F)**
Agriculture	- 43%	33 (91.4)
Developed/Barren	34%	36 (96.8)
Vegetation	11%	33 (91.4)
Water	- 1%	26 (78.8)

Table 5. Summary of LULC changes between the years 2004-2020 and LST for Sejong for 2020

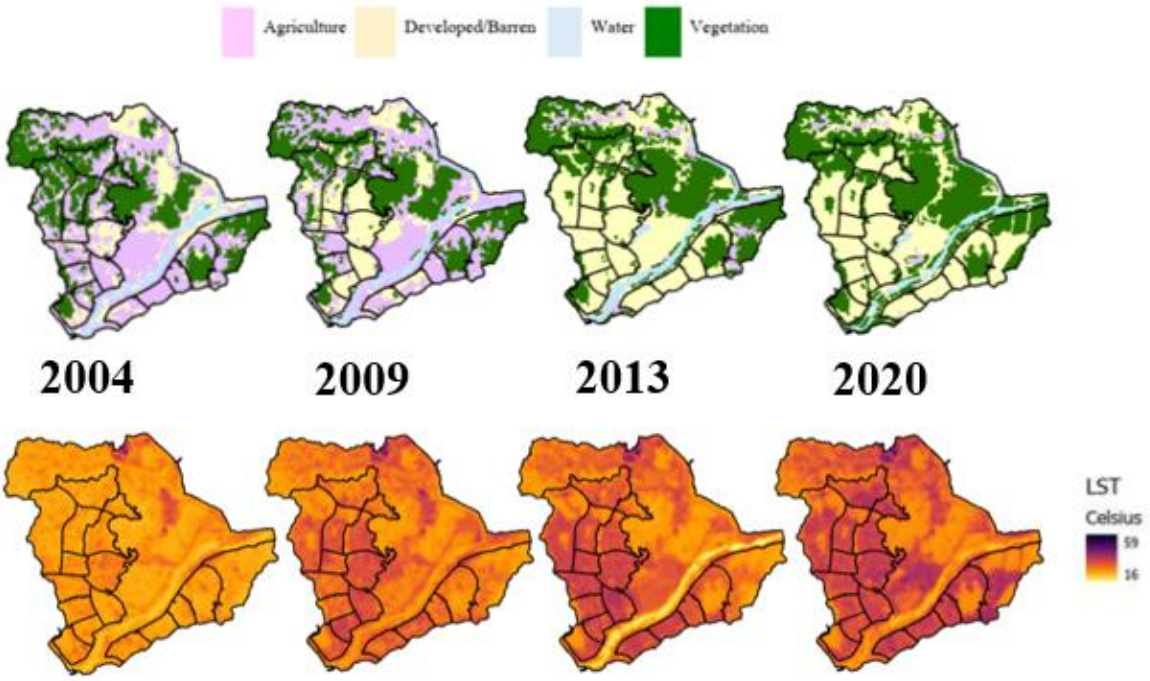

Figure 8. (Top) Land cover classification of Sejong in 2004, 2009, 2013, 2020 (Bottom) and their corresponding land surface temperature maps, respectively

3.3 NDVI and UHI intensity Analysis

Impact of constructed cities on NDVI and UHI intensity

As the cooling effect of green cover is associated with latent heat vaporization, the NDVI has found wide-spread use in studies assessing vegetation cover, including in research focused on UHI. Figure 9-Left presents the NDVI distribution for the urban conversion and rural areas over a 16-year period. The NDVI graph demonstrates that in the urban conversion area, the NDVI values decreased significantly over the 16 years. This is attributed to the LULC changes from green cover to built-up land, as evidenced by the fact that NDVI remained the same for those areas that did not experience LULC changes during the 16 years.

Generally, an NDVI from 0.1 to 0.6 indicates vegetation cover, above 0.6 denotes a dense canopy, below 0.1 indicates bare land soil, and NDVI values below 0.0 represent water (USGS). For the 16-year period under study, the mean NDVI for the rural and urban conversion areas was 0.5 and 0.24, respectively. Based on these results, we can see that despite the impervious nature of the urban area, there is still some greenness, consistent with the design of the city, which incorporated green roofs among other environmental strategies. Finally, the city's northeastern and southeastern areas, with high vegetation cover, had the highest NDVI.

Examining the difference in the NDVI values for the urban conversion and rural areas reveals the extent of greenness loss during the period under investigation due to urbanization (Figure 10-Left). The LST difference graph demonstrates the temperature difference measured in the urban conversion and rural areas between 2004 and 2020 (Figure 10-Right). While the rural areas did not experience any class changes, similar to the LST trend, the NDVI decreased significantly over time in the urban area, therefore there is a significant decrease in the NDVI difference between rural and developing beginning in 2010, which is consistent with the start of construction in 2011. The UHI intensity graph indicates that the urban conversion area was significantly hotter than the rural area during the 2004 to 2020 period (Figure 10-Right). Specifically, the gradient ranges from zero, i.e., no difference in temperature, to slightly over 3°C. This indicates that in 2004, the LST between the urban and rural areas was almost the same. However, this difference increases rapidly from 2010 onwards, presenting gradual changes in the LST peak, implying that land development had taken place. The NDVI difference gradient moves in a manner similar to the UHI intensity graph: In 2004, the areas that are now urban as well as the rural areas had very similar NDVI levels (Figure 9-Right). The Mann-Kendall test confirms the consistent rise in UHI intensity,

corresponding to a decline in NDVI difference throughout the period under study (p-value <2.22e-16).

Urban areas experienced a 1.92°C higher LST on average compared to rural areas. The strongest UHI demonstrated a 3.38°C higher LST and -0.449 lower NDVI compared to the rural areas. In addition, for the vegetation class, the maximum LST change was an increase of 3.38° in 2018, and the NDVI decreased by 0.33 during the same time period. According to the Kendall correlation test, the UHI and NDVI differences have a negative correlation of 0.55.

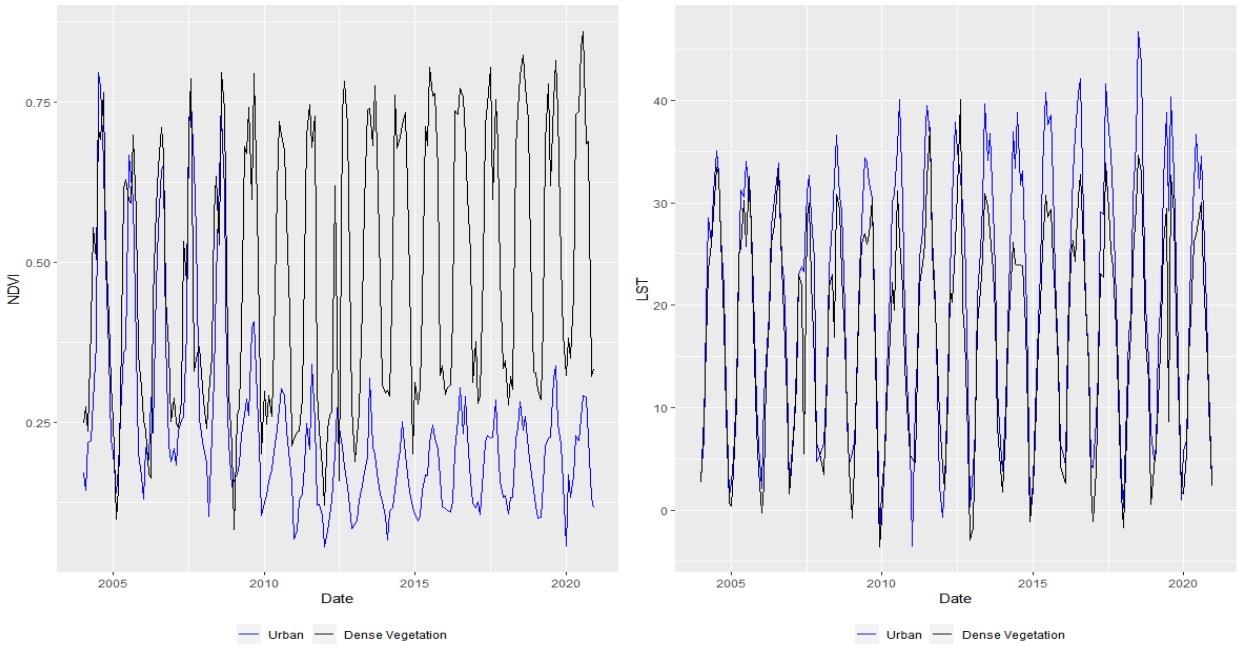

Figure 9. Time series of the day-time MODIS NDVI and LST during the entire study period (2004-2020). (Left) The comparison between rural NDVI (black) and urban conversion NDVI (blue). (Right) LST time series comparison between urban(blue) and rural conversion(black)

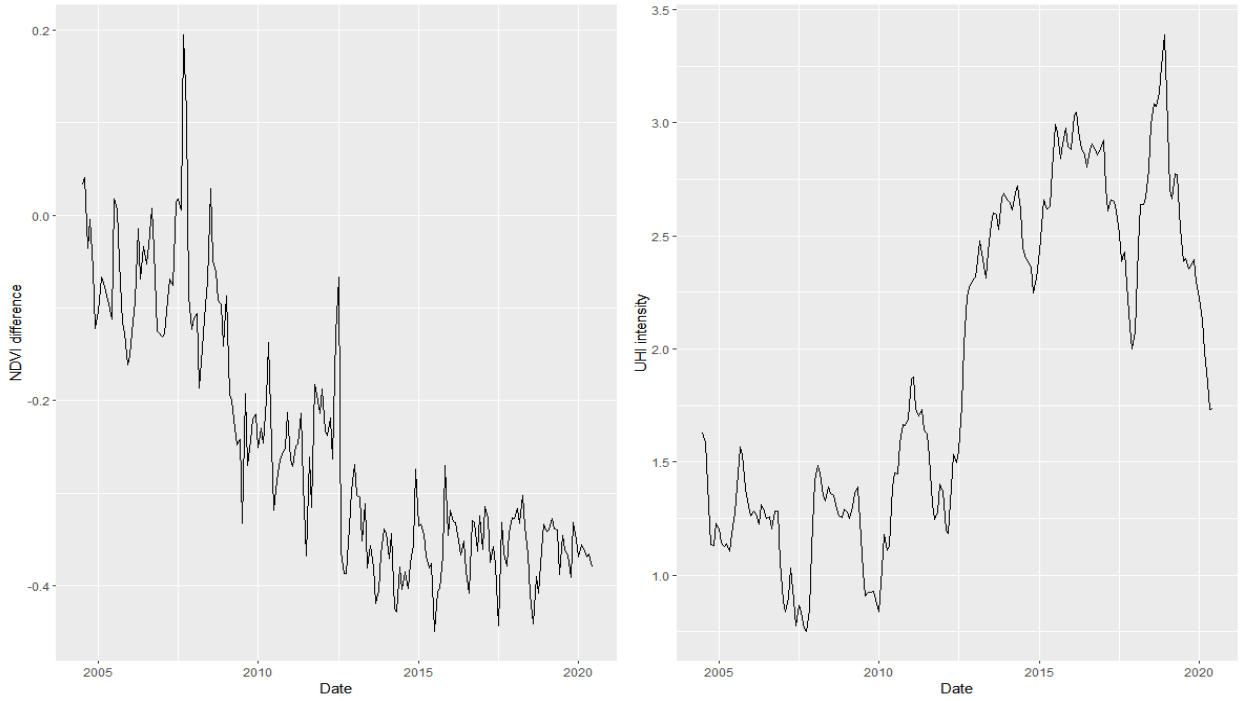

Figure 10. (Left) NDVI variation between urban conversion and rural using the decomposed trend as well as the seasonal components in the MODIS time series. NDVI difference = Urban conversion - Rural averages of the decomposed trends/seasonal component (Right) The UHI intensity using the decomposed trend and seasonal components in the MODIS time series. UHI intensity = Urban conversion -Rural averages of the decomposed trends/seasonal component

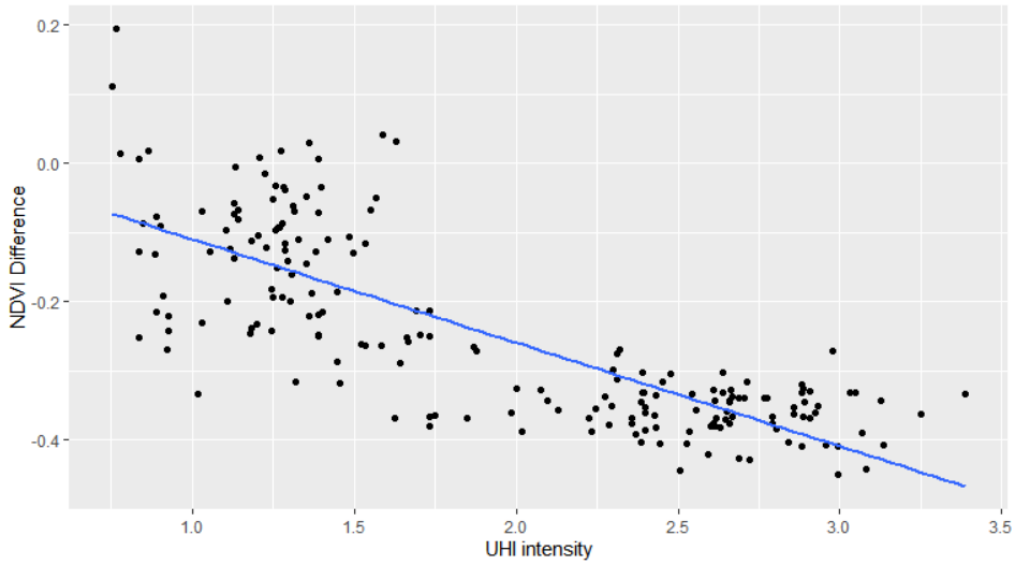

Figure 11. The Kendall correlation analysis of the trend and seasonal patterns of UHI intensity and NDVI difference. NDVI difference = Urban conversion -Rural averages of the decomposed trends/seasonal component. R=-0.55, p<2.2e-16). A negative UHI intensity-NDVI difference correlation is observed through the study period.

3.4 Nighttime LST Analysis

The time of day exhibits different effects of ECOSTRESS-derived LST depending on different land features. In June 2019, the contrast in LST distribution among land features is greater at 10:14am (17.3°C to 24.2°C, difference of 6.9°C) and more stable at 4:43pm (25.9°C to 30.2°C, difference of 4.3°C) (Figure 12). According to the June's analysis of LST of different land features, the vegetation warming from 10:14am to 4:43p.m. exhibits the highest changes in surface temperature (increased by 8.7°C), while the LST of bare soil and water surface have the least temperature fluctuations between day and night (increased by 5.41°C and 6.4°C, respectively). Additionally, vegetation shows relatively cold thermal anomalies during the day but warms much faster than other surfaces (Figure 12).

- In June at 10:14 a.m., LST among different LULC were ranked as follows: Vegetation < Water < Settlements < Barren
- In June at 4:43 p.m., the LST among different LULC were ranked as follows: Water < Vegetation < Barren < Settlements

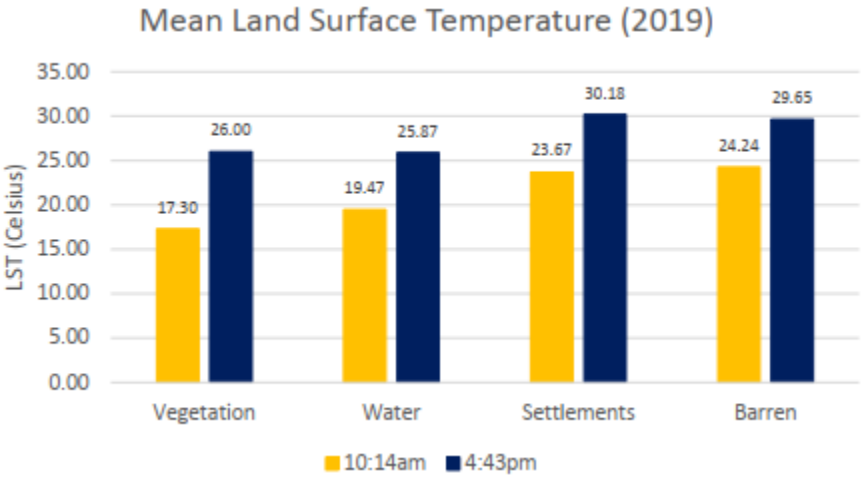

Figure 12. A comparison between 10am and 4pm land surface temperatures for different LULC (June 2019). It shows land surface temperature variation due to changes in time and LULC.

3.4 Recommendation

Figure 13. To investigate the characteristics of the urban heat island intensity among cities in Sejong and the influences of surrounding environments on the urban heat island intensity, Dajung-dong(Red-pinpoint),Nasung-dong(purple-pinpoint), and Eojin-Dong(blue-pinpoint), are selected as urbanized regions.

As the temperature in a single city can show significant variation, merely comparing temperatures in urban areas to those in rural areas nearby is insufficient to develop an understanding of UHI intensity; in addition, nighttime temperatures should also be considered. For example, the mean LST results in 2020 indicate that Dajung-dong had higher LST than Nasung-dong and Eojin-doing, yet these locations have very similar NDVI results. These differences in the LST results could stem from factors in their surrounding environments that diminish UHI intensity, e.g., proximity to a river or forest. Thus, Dajung-dong, situated at the center of Sejong city and far from a river or forest, had the highest temperature. Meanwhile, the coolest temperature was found in Eojin-doing, where the government complex is located. The design of this complex, which covers 3.6 km^2, encompasses the largest rooftop garden in the world, highlighting the potential solution of green

roofs as a way to mitigate increased temperatures in cities. Finally, Nasung-dong g is located closer to an urban river, which may explain its lower LST compared to Dajung-dong.

Locations	NDVI mean 2004 and 2020	Mean LST (2020) Celsius (°C)
Dajung-dong (Red-pinpoint)	0.33	37.47
Nasung-dong (Purple-pinpoint)	0.35	34.14
Eojin-Dong (Blue-pinpoint)	0.36	34.61

Table 6. Mean LST and NDVI values associated with different urban areas for 2020

The abovementioned environmental factors might mitigate the UHI effect by cooling nearby locations. Thus, as it has been established that temperatures tend to vary within urban areas, in the design and construction of cities, there is a need to focus on, for example, areas in the city center or locations expected to have unusually high number of heat-absorbing pavements and buildings. These would benefit from measures such as the installation of green roofs. As a result, there is a need for measures to mitigate the negative effect on the urban environment, especially the adoption of green spaces in both urban and industrial areas. For example, policies could be implemented that promote the installation of green roofs and urban gardens, which would alleviate the increasing UHI trend.

Retrieving land surface temperature and understanding the variation trends of LST in how they are impacted during the daytime and nighttime and how in turn they affect their local climate is important for those living in areas threatened by the possibility of land surface temperature. Thus, identifying hot spots within the area of interest and reporting its intensity and understanding its determining factors, such as environmental conditions, would allow public officials to respond

more effectively to the ongoing crisis by implementing policies addressing ascertaining the UHI reduction.

4. Conclusion

This study investigated how LULC changes affect UHI based on Landsat data showing the LST for Sejong over a 16-year period. The observed LULC changes were quantified into a spatiotemporal pattern across four-time stages and four LULC classes, namely vegetation, development, water, and agriculture. This study subsequently analyzed the LST and NDVI spatiotemporal patterns, the LST changes in relation to the type of LULC, and the LST variation in association with the NDVI. Then, this study analyzed the UHI intensity and NDVI variation using the decomposed trend as well as the seasonal components in the MODIS continuous time series. Finally, this study examines the daytime and nighttime LST for different LULC.

The findings for LULC change show that from 2004 to 2020, the amount of built-up area increased considerably. Based on the LST difference results, the UHI intensity also showed a substantial increase, from 0.75 to 3.38, in the 16-year period. Moreover, the number of high-temperature areas increased at all time stages, attributed to the high rate of urbanization. Overall, the findings suggest that the various LULC types significantly affect temperature, with the increasing urbanization being the primary factor causing the intensifying UHI throughout the study period. It should be noted that the nature of the UHI phenomenon may be related to several factors in addition to LULC type, including other anthropogenic activities, pollution, and the weather.

The land feature absorbs the energy from the sun, leading to an increase in temperature. However, the temperature increase varies owing to the varying specific heat capacities (Li et al., 2021; Trlica et al., 2021; Sharifnezhadazizi et al., 2019). Under the effect of daytime sunlight, settlements and bare soil have the fastest temperature increase, whereas water has a more gradual temperature rise and is characterized by a relatively chilly anomaly (Liu et al., 2021; Zhao et al., 2017). Although I expected a greater temperature variation range among land features; as a whole, the land surface temperatures during the daytime and nighttime of different land features pattern were as expected and consistent with previous studies. This work contributes to UHI mitigation efforts by highlighting the requirement for strategies to take into account the diurnal impacts of land use factors.

References

Adedibu, A. (1987). Environmental Problems of Urbanization in the Third World Countries: Nigeria's Example. *Journal of Third World Studies, 4(1), 170-181.* doi:10.2307/45197047

Appleton, J. (2020, December 3). How The Urban Heat Island Effect Is Harming Our Cities. Bee Smart CityGmbH. https://hub.beesmart.city/en/solutions/how-the-urban-heat-island-effect-is-harming-our-cities

Balali-Mood, M., Ghorani-Azam, A., & Riahi-Zanjani, B. (2016). Effects of air pollution on human health and practical measures for prevention in Iran. *Journal of Research in Medical Sciences, 21(1), 65*. https://doi.org/10.4103/1735-1995.189646

Byrne, M. P., & O'Gorman, P. A. (2013). Land–Ocean Warming Contrast over a Wide Range of Climates: Convective Quasi-Equilibrium Theory and Idealized Simulations. *Journal of Climate*, *26*(12), 4000–4016. https://doi.org/10.1175/jclid-12-00262.1

Chun, B., & Guldmann, J. M. (2014). Spatial statistical analysis and simulation of the urban heat island in high density central cities. *Landscape and Urban Planning*, *125*, 76–88. https://doi.org/10.1016/j.landurbplan.2014.01.016

Data.GO.KR. (n.d.). Data.GO.KR. Retrieved April 16, 2022, from https://www.data.go.kr/dataset/3034207/fileData.do

Deng, Y., Wang, S., Bai, X., Tian, Y., Wu, L., Xiao, J., Chen, F., & Qian, Q. (2018). Relationship among land surface temperature and LUCC, NDVI in typical karst area. *Scientific Reports*, *8*(1). https://doi.org/10.1038/s41598-017-19088-x

Downloads » Global Summer Land Surface Temperature (LST) Grids, v1: Satellite Derived Environmental Indicators | SEDAC. (2013). [Dataset]. https://sedac.ciesin.columbia.edu/data/set/sdei-global-summer-lst-2013/datadownload

Goldblatt, R., Stuhlmacher, M. F., Tellman, B., Clinton, N., Hanson, G., Georgescu, M., Wang, C., Serrano-Candela, F., Khandelwal, A. K., Cheng, W. H., & Balling, R. C. (2018). Using Landsat and nighttime lights for supervised pixel-based image classification of urban land cover. *Remote Sensing of Environment*, *205*, 253–275. https://doi.org/10.1016/j.rse.2017.11.026

Grist. (2021, May 5). In America's cities, inequality is engrained in the trees. https://grist.org/cities/tree-cover-race-class-segregation/

Harmon, K. (2010, July 23). *How Does a Heat Wave Affect the Human Body?* Scientific American. https://www.scientificamerican.com/article/heat-wave-health/

Hook, S., Hulley, G. (2019). *ECOSTRESS Land Surface Temperature and Emissivity Daily L2 Global 70 m V001* [Data set]. NASA EOSDIS Land Processes DAAC.

Accessed 2021-12-10 from
https://doi.org/10.5067/ECOSTRESS/ECO2LSTE.001

Hrisko, J., Ramamurthy, P., & Gonzalez, J. E. (2021). Estimating heat storage in urban areas using multispectral satellite data and machine learning. *Remote Sensing of Environment*, *252*, 112125. https://doi.org/10.1016/j.rse.2020.112125

Kamali Maskooni, E., Hashemi, H., Berndtsson, R., Daneshkar Arasteh, P., & Kazemi, M. (2020). Impact of spatiotemporal land-use and land-cover changes on surface urban heat islands in a semiarid region using Landsat data. *International Journal of Digital Earth, 14(2), 250–270.* https://doi.org/10.1080/17538947.2020.1813210

Kim, S. W., & Brown, R. D. (2021). Urban heat island (UHI) intensity and magnitude estimations: A systematic literature review. *Science of The Total Environment*, *779*, 146389. https://doi.org/10.1016/j.scitotenv.2021.146389

Kim, Y. H., & Baik, J. J. (2005). Spatial and Temporal Structure of the Urban Heat Island in Seoul. *Journal of Applied Meteorology*, *44*(5), 591–605. https://doi.org/10.1175/jam2226.1

Korean Meteorological Administration. Retrieved April 19, 2022, from https://data.kma.go.kr/data/grnd/selectAsosRltmList.do?pgmNo=36

Jin Aik, D., Ismail, M. H., & Muharam, F. M. (2020). Land Use/Land Cover Changes and the Relationship with Land Surface Temperature Using Landsat and MODIS Imageries in Cameron Highlands,
Malaysia. *Land, 9(10), 372*. https://doi.org/10.3390/land9100372
Learn About Heat Islands. (2020, July 30). US EPA. https://www.epa.gov/heatislands/learn-about-heat-islands

Li, X., Guo, W., Li, S., Zhang, J., & Ni, X. (2021). The different impacts of the daytime and nighttime land surface temperatures on the alpine grassland phenology. *Ecosphere*, *12*(6). https://doi.org/10.1002/ecs2.3578

Liu, W., Meng, Q., Allam, M., Zhang, L., Hu, D., & Menenti, M. (2021). Driving Factors of Land Surface Temperature in Urban Agglomerations: A Case Study in the Pearl River Delta, China. *Remote Sensing*, *13*(15), 2858. https://doi.org/10.3390/rs13152858

Manoli, G., Fatichi, S., Schläpfer, M., Yu, K., Crowther, T. W., Meili, N., Burlando, P., Katul, G. G., & BouZeid, E. (2019). Magnitude of urban heat islands largely explained by climate and population. Nature, 573(7772), 55–60. https://doi.org/10.1038/s41586-019-1512-9

Maria, V., Rahman, M., Collins, P., Dond, G., & Sangiorgi, C. (2013). Urban Heat Island Effect: thermal

response from different types of exposed paved surfaces. *Chinese Society of Pavement Engineering*, 1–9. http://www.ijprt.org.tw/reader/pdf.php?id=327

Measuring Vegetation (NDVI & EVI). (n.d.). USGS. https://earthobservatory.nasa.gov/features/MeasuringVegetation#:%7E:text=The%20most%20common%20measurement%20is,rainforests%20(0.6%20to%200.8).

National Geographic Society. (2012, October 9). *urban heat island.* https://www.nationalgeographic.org/encyclopedia/urban-heat-island/

O'Brien, J. (2021, June 4). *Why warm temperatures at nighttime can be dangerous*. Yale Climate Connections. https://yaleclimateconnections.org/2021/06/why-warmtemperatures-at-nighttime-can-be-dangerous/

Pal, S., & Ziaul, S. (2017). Detection of land use and land cover change and land surface temperature in English Bazar urban centre. *The Egyptian Journal of Remote Sensing and Space Science*, *20(1)*, 125–145. https://doi.org/10.1016/j.ejrs.2016.11.003

Quan, J., Zhan, W., Chen, Y., Wang, M., & Wang, J. (2016). Time series decomposition of remotely sensed land surface temperature and investigation of trends and seasonal variations in surface urban heat islands. Journal of Geophysical Research: Atmospheres, 121(6), 2638–2657. https://doi.org/10.1002/2015jd024354

Sejong City. (n.d.). Retrieved April 16, 2022, from https://www.sejong.go.kr/eng/sub01_0205.do
Tan, J., Yu, D., Li, Q., Tan, X., & Zhou, W. (2020). Spatial relationship between land-use/land-cover change and land surface temperature in the Dongting Lake area, China. *Scientific Reports*, *10*(1), 9245. https://doi.org/10.1038/s41598-020-66168-6

Sejong, KR Climate Zone, Monthly Weather Averages and Historical Data. (n.d.). Weather and Climate. Retrieved April 19, 2022, from https://tcktcktck.org/south-korea/sejong

Sharifnezhadazizi, Z., Norouzi, H., Prakash, S., Beale, C., & Khanbilvardi, R. (2019). A Global Analysis of Land Surface Temperature Diurnal Cycle Using MODIS Observations. *Journal of Applied Meteorology and Climatology*, *58*(6), 1279–1291. https://doi.org/10.1175/jamc-d-18-0256.1

Survey, U.-U. G. (2018). *EarthExplorer* [Dataset]. https://earthexplorer.usgs.gov/

Thanh Hoan, N., Liou, Y. A., Nguyen, K. A., Sharma, R., Tran, D. P., Liou, C. L., & Cham, D. (2018). Assessing the Effects of Land-Use Types in Surface Urban Heat Islands for Developing Comfortable Living in Hanoi City. *Remote Sensing, 10(12), 1965.* https://doi.org/10.3390/rs10121965

Trlica, A., Hutyra, L. R., Schaaf, C. L., Erb, A., & Wang, J. A. (2017). Albedo, Land Cover, and Daytime Surface Temperature Variation Across an Urbanized

Landscape. *Earth's Future*, *5*(11), 1084–1101. https://doi.org/10.1002/2017ef000569

Tzavali, A., Paravantis, J., Mihalakakou, G., Fotiadi, A., & Stigka, E. (2015). Urban Heat Island Intensity: A Literature Review. *Fresenius Environmental Bulletin*, 4537. https://www.researchgate.net/publication/298083233_Urban_heat_island_intensity_A_literature_review

Urban heat island | World Meteorological Organization. (n.d.). World Meteorological Organization. Retrieved April 16, 2022, from https://community.wmo.int/activity-areas/urban/urban-heat-island

Urban Heat Islands | UCAR Center for Science Education. (n.d.). UCAR. Retrieved April 7, 2021, from https://scied.ucar.edu/learning-zone/climate-change-impacts/urban-heat-islands

Urban population (% of total population) | Data. (2019). The World Bank. https://data.worldbank.org/indicator/SP.URB.TOTL.IN.ZS

Urban population growth. (n.d.). The World Health Organization (WHO). Retrieved June 4, 2021, from https://www.who.int/gho/urban_health/situation_trends/urban_population_growth/en/

Urbanization: An Environmental Force to be Reckoned With. (2004). PBR. https://www.prb.org/urbanizationan-environmental-force-to-be-reckoned-with/

Urbanization Planning of Seoul. (2016, December 19). Seoul Solution. https://www.seoulsolution.kr/en/content/urbanization-planning-seoul

Wang, J., Chen, Y., Liao, W., & He, G. (2021). Anthropogenic emissions and urbanization increase risk of compound hot extremes in cities. *Nature Climate Change*. Published. https://doi.org/10.1038/s41558-021-01196-2

Yang, P., Ren, G., & Liu, W. (2013). Spatial and Temporal Characteristics of Beijing Urban Heat Island Intensity. *Journal of Applied Meteorology and Climatology*, 52(8), 1803–1816. https://doi.org/10.1175/jamc-d-12-0125.1

Yoo, C., Park, S., & Cho, C. (2019). Analysis of Thermal Environment by Urban Expansion using KOMPSAT and Landsat 8: Sejong City. *Korean Journal of Remote Sensing, (35(6_4)), 1403–1415.* https://doi.org/10.7780/kjrs.2019.35.6.4.9

Zhao, G., Dong, J., Liu, J., Zhai, J., Cui, Y., He, T., & Xiao, X. (2017). Different Patterns in Daytime and Nighttime Thermal Effects of Urbanization in Beijing-TianjinHebei Urban Agglomeration. *Remote Sensing*, *9*(2), 121. https://doi.org/10.3390/rs9020121

Zheng, Y., Ren, C., Xu, Y., Wang, R., Ho, J., Lau, K., & Ng, E. (2018). GIS-based mapping of Local

Climate Zone in the high-density city of Hong Kong. *Urban Climate*, *24*, 419–448. https://doi.org/10.1016/j.uclim.2017.05.008